CASPER[1,2]

A mission to study the time-dependent evolution of the magnetic solar chromosphere and transition regions

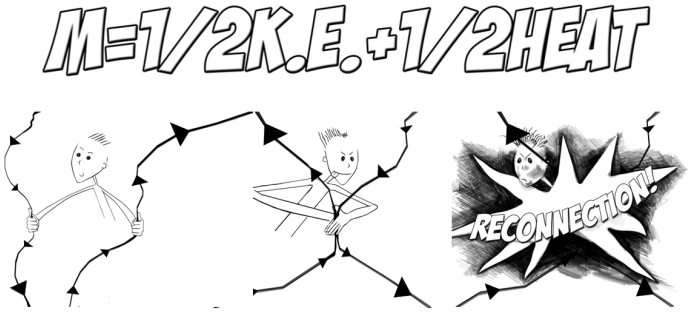

Contact Scientist: David Orozco Suárez

Instituto de Astrofísica de Andalucía (IAA-CSIC) - Solar Physics Group

Glorieta de la Astronomía s/n, Granada E-18008, Spain. Phone: +34 958230641. Email: orozco@iaa.es

1. Executive summary

Our knowledge about the solar chromosphere and transition region (TR) has increased in the last decade thanks to the huge scientific return of space-borne observatories like SDO, IRIS, and *Hinode* and suborbital rocket experiments like CLASP I and II and Hi-C. However, the magnetic nature of those solar regions remain barely explored. The chromosphere and TR of the Sun harbor weak fields and are in a low ionization stage both having critical effects on their thermodynamical behavior. Relatively cold gas structures such as spicules and prominences are located in these two regions and display a dynamic evolution in high-resolution observations that static and instantaneous MHD models are not able to reproduce. The role of the chromosphere and TR as the necessary path to a (largely unexplained) very hot corona calls for the generation of observationally based, time-dependent models of these two layers that include essential, up to now disregarded, ingredients in the modeling such as the vector magnetic field. The community is convinced that the origin of both the heat and kinetic energy observed in the upper layers of the solar atmosphere is of magnetic origin but reliable magnetic field measurements are missing. The access to sensitive polarimetric measurements in the ultraviolet wavelengths has been elusive until recently to technology. We propose a **low-risk and high-Technology Readiness Level mission** to explore the **magnetism and dynamics of the solar chromosphere and TR.** The mission baseline is a low-Earth, Sun-synchronous orbit at an altitude between 600 and 800 km. The proposed scientific payload consists of a 30 cm aperture telescope with a spectropolarimeter covering the **hydrogen Ly-alpha** and the **Mg II h&k ultraviolet lines.** The instrument shall record **high-cadence, full spectropolarimetric observations** of the solar upper atmosphere. Besides the answers to a fundamental solar problem the mission has a broader scientific return. For example, the time-dependent modeling of the chromospheres of stars harboring exoplanets is fundamental for estimating the planetary radiation environment. **The mission is based in technologies that are mature enough for space and will provide scientific measurements that are not available by other means**.

[1] In response to: Call for White Papers for the ESA's Voyage 2050 Science Program

[2] From Chromosphere And transition region Solar Polarimetric ExploreR

2. Team members

IAA-CSIC	NAOJ	IAC
David Orozco Suárez	Ryohko Ishikawa	Javier Trujillo Bueno
Jose Carlos del Toro Iniesta	Yukio Katsukawa	Andrés Asensio Ramos
Francisco Javier Bailén	Ryouhei Kano	Tanaosu del Pino Alemán
Antonio López Jiménez	**ISAS-JAXA**	
María Balaguer Jiménez	Toshifumi Shimizu	
Luis Ramón Bellot Rubio		

IAA-CSIC: Instituto de Astrofísica de Andalucía-Consejo Superior de Investigaciones científicas (Spain)
IAC: Instituto de Astrofísica de Canarias (Spain)
NAOJ: National Astronomical Observatory of Japan (Japan)
ISAS-JAXA: Institute of Space and Astronautical Science, Japan Aerospace Exploration Agency (Japan)

3. Scientific goals of the CASPER mission

Building **fully consistent chromospheric and TR time-dependent models** including information about the magnetic field configuration and the plasma dynamics is critical for a thorough understanding of the outermost layers of the Sun and for gaining new physical insights about the energy balance between these layers and the photosphere and corona. The solar chromosphere and TR of the Sun are extremely dynamic and harbor a large variety of physical phenomena such as waves and jets [e.g., Katsukawa et al. 2007; De Pontieu et al. 2007a]. All these events take place exactly in the region where the plasma goes from being fully governed by thermodynamical processes to being dominated by magnetic fields and whose physical conditions are better seen in the ultraviolet (UV), which cannot be observed from the ground. Moreover, non-local and non-thermal equilibrium effects dominate the formation of atomic line transitions, what makes it difficult the interpretation of the observed signals that require complex radiative transfer calculations assisted by sophisticated simulations.

Modelers have first attempted to simulate the upper solar atmosphere with one-dimensional models [e.g., Avrett et al. 2015], which included many but not all the physical ingredients. Later, sophisticated magnetohydrodynamic simulations [e.g., Gudiksen et al. 2011] were used as a test bench for understanding solar observations. However, such analyses are strongly limited because current observations have not yet provided enough constraints about **how the magnetic field is organized** in the upper layers. Zeeman based measurements in the chromosphere are fruitless because the fields are usually weak and the Doppler broadening is large enough to hinder Zeeman diagnostics. Moreover, although **non-thermal equilibrium effects** are partly taken into account in the modeling [e.g., Carlsson & Stein 2002], current observations have not yielded any boundary conditions to those dynamic phenomena associated with the different ionization and recombination times. Non-thermal equilibrium effects can be a key ingredient to explain the source of non-radiative heating of the upper solar atmosphere in a layer fully dominated by dynamics and magnetic fields. These effects, however, are usually disregarded from the observational point of view.

Conversely, **dissipation of magnetic fields** may be the primary heat source in the chromosphere and TR. Current sheets can "naturally" be generated in the solar atmosphere simply by the continuous evolution of the magnetic field topology. Those regions are where dissipation of magnetic field occurs in a natural way through reconnection. Proving the validity of such hypothesis is a fundamental issue for solar and stellar physics. Indeed, the release of energy in the chromosphere and TR **impacts local UV irradiance measurements** whose time variations (usually up to 400 nm) are considerably larger than those corresponding to the total solar irradiance. Irradiance variations are associated to the solar activity cycle and have a profound effect on Earth's atmosphere. Hence, for the reasons above, it is time for exploring in depth the thermodynamical and magnetic properties of the solar plasma through **high spatial and spectral resolution spectropolarimetric observations** in the UV spectral region, in parallel with other current space missions such as IRIS, and rocket experiments such as CLASP-I and II but adding full polarization measurements.

The optimum spectral lines that are useful for diagnosing the solar chromosphere and TR are **the Mg II h&k lines at 280.270 and 279.553 nm and the hydrogen Ly-alpha line at 121.567 nm**, both of them in the near-UV region of the spectrum. Optionally, the nearby Ca II H&K lines at 396.817 and 393.366 nm could be added to the setup. There is a number of reasons **why these two spectral lines** are perfect candidates for exploring the dynamics and magnetism of the chromosphere and TR using a space-based observatory:

(i) These lines, when observed on the solar disk, usually show broad photospheric absorption wings and core emission peaks which provide fundamental ingredients for diagnosing the thermal and density structure of the solar atmosphere, from the photosphere (seen in, e.g., the Mg II k wings) through the chromosphere and to the TR (Ly-alpha core). Particularly, the Mg II h&k lines are perhaps **the only available spectral lines** to get information about the thin region between the upper chromosphere and the TR.

(ii) They are useful for the observation of off-the-limb solar structures, such as prominences, spicules, coronal loops or polar plumes. Remarkably, the Ly-alpha line is optically thin in the solar corona and the strongest emission line there which makes it specially suitable for coronal magnetic field measurements [Khan et al. 2011].

(iii) The Mg II h&k and Ly-alpha lines are located below the UV-Earth atmosphere cut, so that they are **only accessible from space**. The Ca II H&K UV lines are still accessible from the ground and therefore they remain as an add-on to the mission.

(iv) It is now possible to get information about the magnetic field using these lines because they are sensitive to the presence of **atomic level polarization and to the joint action of the Hanle and Zeeman effects** what make them especially suitable for the determination of the magnetic configuration in many chromospheric and TR solar structures [see the review on the diagnostic potential of UV spectropolarimetry by Trujillo Bueno et al. 2017]. The Hanle effect in transition region lines is sensitive to relatively strong fields, going from 10 to 100 Gauss in the case of the Ly-alpha line [Trujillo Bueno, Štěpán & Casini 2011]. This spectral line generates measurable scattering polarization signals, both at its core [Trujillo Bueno et al. 2011, Štěpán et al. 2015] and in their wings [Belluzzi, Trujillo Bueno, Štěpen 2012]. In contrast, the Hanle sensitivity of the Mg II k line is between 10 and 50 Gauss. These lines produce clear circular polarization signals (above 1%) for longitudinal fields of about 50 G [Belluzzi & Trujillo Bueno 2012]. Moreover, the Mg II h&k and the hydrogen Ly-alpha wings show sensitivity to magnetic fields through the magneto-optical effects that couple Stokes Q and U [Alsina Ballester, Belluzi & Trujillo Bueno 2016, 2019; del Pino Alemán,

Casini & Manso Sainz 2016] and the transfer equations [Alsina Ballester, Belluzi & Trujillo Bueno 2017, 2018].

(v) This spectral region allows a continuous monitorization of the chromosphere and TR UV irradiance and of energetic phenomena contributing to it such as magnetic reconnection. Hence, these lines are perfect candidates for tracing reconnection events in the chromosphere and TR.

There are other spectral lines which could also be used for diagnosing the chromosphere and some plasma structures like spicules. These are, for instance, the Ca II infrared triplet and the He I 1083 nm and D_3 multiplet lines. Both are accessible from the ground and require telescope diameters above one meter to reach 0.3" spatial resolution. The Sunrise III balloon-borne mission (programed for summer 2021) will observe the Ca II infrared triplet lines from an altitude of about 40 km. The Mg II h&k resonance lines have higher opacity and larger sensitivity to temperature than the subordinate lines of the Ca II IR triplet. Moreover, the core of the Mg II lines form much closer to the TR where the most dramatic physical events take place. Regarding the He I 1083 nm and D_3 multiplet lines, it is believed that these are the only ones than can be used for reliable magnetic field measurements in the chromosphere. However, these lines are most of the time optically thin and barely seen on the quiet solar granulations, except in prominences, active regions, and spicules. Moreover, they are very sensitive to coronal UV irradiation which makes them useless for temperature diagnostics. The Daniel K. Inouye Solar Telescope (DKIST) with its 4-meter aperture, will take measurements from almost the whole spectrum except in the ultraviolet [Elmore et al. 2014]. DKIST lacks the continuous monitoring and “seeing” stability of space observations and its diagnostic potential weakness is actually the lack of TR region measurements in the UV. This is also the situation for any other ground based solar observatory. Hence, it is fundamental to coordinate space-based UV measurements with groundbreaking instruments of other observatories and seek for multi-wavelength observations. This will significantly increase the science return.

In space, several missions have had access to the solar UV part of the spectrum. The Solar dynamic observatory (SDO) and Stereo missions are providing invaluable information about the evolution of the solar corona with narrow-band filter measurements in the 100-300 Angstroms range. This measurements reached one arc-second resolution and are fundamental for understanding the solar corona global and local dynamics and cycle but lack from spectral or polarimetric diagnostics. The SUMER/SOHO instrument provided the first hydrogen Ly-alpha profile measurements. More recently, the IRIS mission (still operating [De Pontieu et al. 2014]) and the sounding-rocket CLASP experiments (with two successful flights in 2015 and 2019) have provided good observations. However, they have limitations. IRIS does not have the possibility to measure the degree of polarization while the CLASP observations are too short in duration as for providing useful data for the time-dependent modeling of the upper solar atmosphere. Unquestionably, the CASPER mission is fed and inspired by the CLASP observational discovery of the linear polarization produced by scattering processes in the Ly-alpha line [Kano et al. 2017] and its theoretical modeling [Trujillo Bueno et al. 2018]. CLASP represents a big step forward since it also confirmed that the target UV spectral lines are sensitive and useful for determining the magnetism of the chromosphere and TR. Presently, **CLASP measurements are paving the way to build robust diagnostics** in order to obtain reliable vector magnetic field measurements from UV observations. The next natural step is therefore to perform such observations routinely and from space. Anyhow, it is important to bear in mind that the UV polarization signals are usually small, between 0.1% and 1% of the local continuum intensity. Hence, the observations **require high signal-to-noise ratios to detect polarization.** This is a strong requirement that fully drives the instrument conceptual design and the final spatial and spectral resolution since, in the UV, the available photon budget is limited and the opti-

cal elements and detectors are usually less efficient. Beside CLASP, it is also worth mentioning the forthcoming Sunrise III mission which will carry a spectropolarimeter in the UV. However, even at the flight attitudes of Sunrise (around 40 km) the UV absorption below 300 nm is still strong. Sunrise will limit its observed spectral region to 300-430nm. CASPER measurements will complement Solar Orbiter and Parker Solar Probe missions since they observe the Sun from close distances and different points of view, which will enhance their scientific return.

CASPER measurements will allow continuous and unique spectral line polarization measurements in the near-UV which will improve our knowledge of the magnetic fields in the chromosphere and TR. From the measurements of the Stokes profiles and their interpretation via the physics of scattering polarization and the Hanle effect, we will be able to better determine the variation of the vector magnetic field with height above the solar limb in solar spicules and further characterize their dynamic properties. This can be done with a 30 cm diameter telescope working at a limited resolution of 0.3". Resolution in the chromosphere and TR is not a limiting factor since the photon mean free path in the chromosphere is much larger than in the photosphere below, so it is not expected to see much small-scale structuring below 0.2".

Measurements in the UV will be critical to solve the problem of the large discrepancies between UV measurements and models of the solar irradiance [e.g., Ermolli 2013], particularly in the 200-400 nm spectral range. CASPER measurements will significantly improve current solar models by including the time-evolution of the chromospheric UV radiation. Finally, CASPER measurements will also be important for understanding other star's chromospheres and their influence in exoplanetary atmospheres: UV emission, particularly in the Ly-alpha line, drives photochemical reactions in exoplanetary atmospheres [e.g., Salz et al. 2016]. This space mission is highly interdisciplinary since it requires cooperative observations with instruments attached to ground and space solar telescopes and the interpretation of the data using cutting-edge inversion codes based on complex radiative transfer and quantum mechanics. Table 1 shows the main goals of the mission CASPER. The main scientific goals of the mission are described in more detail in what follows:

3.1. Main science questions

[Goal 1.1] T<u>ime-dependent behavior of the solar chromosphere and TR</u>

The chromosphere and TR regions of the Sun are very dynamic and fully dominated by the magnetic field. It is urgently needed to update and extend the physics contained in current semi-empirical (snapshot) models and in those generated through hydrodynamic and magnetohydrodynamic (MHD) simulations, including realistic chromospheric and TR vector magnetic field measurements. The objective is to generate time-dependent models of the chromosphere and TR through the observation of chromospheric small and large scale structures in the solar disk and at the limb with high signal-to-noise ratio. A high polarimetric precision (better than 10^{-3} in units of the continuum intensity) is needed to achieve that goal. The recommended observing targets are, among others, chromospheric fibrils, dark and bright mottles. The observations shall be carried out with high spatial resolution (~0.3"), low cadence, and with large fields of view (FoV).

Temperatures, densities, and magnetic fields models as a function of depth in the solar atmosphere shall be obtained with the aid of full NLTE inversion codes that incorporate the physics of the Zeeman effect, of scattering polarization, and of the Hanle effect. CASPER measurements will provide new, time-dependent models of the solar chromosphere and TR regions for various chromospheric structures to be compared with state-of-the-art MHD simulations. Current simulations provide allegedly realistic information on the thermodynamics of the solar atmosphere but they lack observational information about the chromospheric and TR vector magnetic field.

Science Objective	Science Questions	Observing Strategy and targets	Field of View	Spatial Resolution	Image Cadence	Polarimetric Sensitivity	Needs	Expected Scientific Results
Characterize the thermodynamic and magnetic properties of solar chromosphere and transition region	**1.1) What is the thermal and magnetic structure of the solar chromosphere and transition region?**	Observe chromospheric small and large scale structures in the solar disk and off limb	150"x150"	0.3" to resolve fine scale structures	Slow: 1 min	High $1x10^{-3}$ - $3x10^{-4}$	Infer termperatures and magnetic fields as a function of depth with inversion codes. Comparison with 1D and 3D MHD models.	Update time-dependent chromopheric and TR models. Measurments of magnetic fields in chrom. and TR lines.
	1.2) How non-equilibrium effects influence the solar chromosphere and trasition region dynamics?	Observe different atom types trasitions (neutral and ionized). Mainly off limb	sit-and-stare	<0.3"	Fast: 1 s - 10 s	Low $1-3x10^{-3}$	Determine velocities between different atom transition types	Understanding of non-equilibrium ionization effecs
	1.3) What is the energy balance between the photosphere and its upper layers?	Observe chromospheric small scale emergence events in the solar disk	10"x150"	0.3" to 1"	30 sec to 1 min	High $1x10^{-3}$ - $3x10^{-4}$	Determination of the topology of flux tubes and of the emergence and cancellation rates.	Constraints on the chromosphere and coronal heating problem
	1.4) How is the magnetic field organized at small-scales in prominences and spicules?	Observe off-limb prominences and spicules. Continuous monitoring for time evolution	minimum 10"x10" for scipules	<0.3" to resolve fine scale structures	10 sec - 1 min	High $1x10^{-3}$ - $3x10^{-4}$	Determine velocities and magnetic fields using inversion codes.	Constraints on spicular models and small-scale field organization in prominences
	1.5) How do waves propagate and interact with the solar upper layers?	Observe the propagation of MHD and Alvén waves along the foot points of fibrils and jets. Continuous monitoring for time evolution.	narrow to moderate 1"-10"	<0.3" to resolve fine scale structures	10 sec	Moderate $1x10^{-3}$	Identify and characterize waves. Determine the energy rate converted from waves into heat.	Identification of waves driving mechanims and incluence in the heating
	1.6) What is the energy balance and dynamics of flares and nano-flares?	Observe small and large scale flare events.	any	0.3" to 1"	Fast: 1 s - 10 s	Moderate $1x10^{-3}$	Determine temperatures and magnetic fields during and after reconnection proceses.	Understanding of reconnection events in the solar atmosphere. Formation of coronal loops.

Table 1: CASPER science objetives

[Goal 1.2] Dynamics of the solar atmosphere: time-dependent ionization of lines

The chromosphere and TR are made up of weakly ionized gases. Ions and neutrals experience different forces within the gas. For instance, neutrals do not "feel" the magnetic field while ions are fully dominated by it. Both are coupled mainly by collisions but not fully. In other words, ions and neutrals should show differential motions in a weakly ionized plasma. Of course, the gas will be more "single"-fluid or multi-fluid depending on physical conditions such as the ionization fraction, the temperature, the density, and the magnetic field. The latter governs the movements of electrons (in a weak collision environment), which play a significant role in various heating mechanisms. Moreover, in the chromosphere and TR of the Sun most atoms are in non-thermal equilibrium. That is, they ionize and recombine at different rates. In short, the chromosphere and TR physical properties can change dramatically in the ~ 3000 Km height they cover. Such variability gives rise to significantly different physical phenomena (that are indeed observed). Moreover, partly ionized plasmas can alter fundamental processes taking place in the solar atmosphere such as magnetic reconnection [Ni et al. 2018] [Goal 1.6]. The observation and characterization of the solar plasma from a multiple fluids perspective can provide unique physical ingredients for the proper modeling of the upper solar layers. It can be done through the measurement of temperatures, densities, velocities and magnetic fields in different atomic species in order to understand the interplay between two plasmas.

[Goal 1.3] Determine the energy balance of the solar chromosphere and TR

There are a number of processes in the solar atmosphere that can potentially inject substantial amounts of energy into the chromosphere and TR. Flux emergence processes constitute one of the most firm candidates to explain the energy balance between the photosphere and the layers above. Flux emergence occurs all around the solar surface and at many spatial scales, from active regions to small scale loops. It is known that internetwork flux emergence events carry about four orders of magnitude more magnetic flux into the chromosphere than active regions [e.g., Martínez Gonzalez & Bellot Rubio, 2009; Gòsic 2016]. This is possible because these events take place ubiquitously in the quiet Sun. Hence, we should characterize the thermal, dynamic, and magnetic field properties of those small-scale loops while they cross the chromosphere and transition region. The recommended observing target is quiet Sun regions, at different limb positions. The observations shall be carried with high spatial resolution and moderate temporal resolution over narrow FoVs to track the evolution of emerging loops. The observations should allow to determine how the energy carried out by these structures is released. The most probable mechanism is magnetic reconnection with preexisting magnetic field structures (see [Goal 1.6]). This way, there will be a continuous conversion of magnetic energy into thermal energy in the chromosphere. However, it is not understood how the magnetic energy is dissipated as a whole since emergence events have been barely studied in the upper layers [e.g., Ortiz et al. 2016]. Waves may also play an important role for the energy release (see [Goal 1.5]). The study of other events, such as the in-situ disappearance of flux or the unipolar emergence of flux, waves, turbulent diffusion, or Ellerman bombs, etc. are also of great interest since their analysis can improve our understanding about how energy is released in the solar chromosphere. They are probably providing only a small part of the heating, though. These observations need simultaneous (coordinated with, e.g., DKIST, the German GREGOR telescope in the Observatory de Izaña or the Swedish Tower Telescope in the Observatory of La Palma, to name a few) observations in other spectral lines in the visible and the infrared in order to study the appearance of the events in the photosphere and their posterior evolution through the different atmospheric layers.

[Goal 1.4] Characterization of solar prominences and spicules

The characterization of the magnetic configuration of solar filaments and prominences (filaments seen against the background sky of the solar limb) is of paramount importance for solar and stellar physics. They are prominent plasma structures that extend from the solar surface into the hot solar corona. Their characterization is crucial for understanding the magnetic coupling between the photosphere, chromosphere, TR, and corona. These structures are anything but static. They show an intricate organization into fine-scale threads that are highly dynamic [Okamoto et al, 2007]. They also show magnetic processes such as the magnetic Rayleigh-Taylor instability, which is still not well understood [Berger et al, 2008; Hillier et al., 2012]. Excellent observations taken with the Hinode satellite have revolutionized our knowledge on prominence structure and, particularly, on prominence dynamics: plasma oscillations, supersonic downflows, or plasma instabilities like the Rayleigh-Taylor instability in prominence bubbles are main breakthroughs [Chae et al. 2008; Ryutova et al. 2010; Berger et al. 2010; Berger, Testa, Hillier, et al. 2011]. Unfortunately, the measurements of magnetic fields in prominences are still limited and even unavailable at spatial resolutions comparable to that achieved by the Hinode spacecraft. Indeed, up to date, there are no observational constraints on the **magnetic properties of their fine-scale structure** [e.g., Orozco Suárez et al. 2012, Martínez González et al. 2015, Díaz Baso et al. 2016]. Hence, it is of paramount importance to observe solar filaments in the chromosphere and TR of the Sun to characterize in quantitative detail their magnetic structure, to follow their evolution, to investigate their influence in the magnetic coupling between the different solar layers, and finally, to determine the possible triggering mechanisms behind the prominence and filaments destabilization and the posterior formation of coronal mass ejections. With the application of inversion codes to the proposed observations using the target spectral lines, it will be possible to infer, for the first time, the local 3D magnetic configuration in solar filaments.

Likewise, most of the chromospheric material in the upper layers of the solar chromosphere and TR is in the form of spicules. Associated with the boundaries of network regions [e.g. Sekse et al. 2012, 2013], the role of magnetic fields in the formation and development of spicules is still under debate [e.g., De Pontieu et al. 2004]. The main reason is that the magnetic properties of spicules are not well constrained yet. As in prominences, solar ground-based and space-borne observatories have significantly contributed to the understanding of the spicule dynamics [e.g., De Pontieu et al. 2007b; Tavabi et al. 2011; Pereira et al. 2012; Pereira et al. 2016], but the characterization of their vector magnetic field remains very challenging. We know that the fields in spicules are weak and slightly tilted with respect to the limb [Centeno et al. 2010; Orozco Suárez et al. 2015] but still the information is very limited. A comparison of current spicular models with the observations [Martínez-Sykora et al. 2017] is needed. Spectropolarimetric measurements are necessary at high spatial resolutions in chromospheric and TR UV lines to characterize the vector magnetic field of solar spicules and to carry out a statistical analysis of their dynamic and magnetic properties at different latitudes and different heights above the visible limb.

[Goal 1.5] Characterization of chromospheric and TR waves

It is of vital importance to observe and understand the propagation of waves and plasma turbulent motions. Waves may dissipate or absorb substantial amounts of energy but the direct detection of such processes remains elusive to solar observations [cf. Okamoto et al. 2015, Antolin et al. 2015]. Observing and determining the energy these waves carry as a function of height in the solar chromosphere and TR regions can help improve current, yet barely constrained, wave models. Moreover, the study of waves and their relation with the magnetic field is a key ingredient to

properly model chromospheric and TR flux tubes. Waves are also present in solar prominences. One of the CASPER objectives is to detect waves at different heights, at the foot points of coronal loops and in network flux tubes. Magnetic flux tubes can behave as channels that transmit energy from the deeper layers upwards through the propagation of waves. These waves, once in the chromosphere and TR produce shocks and release energy. CASPER observations will help determine the frequency and energy density of waves. The observations require time-series of around 10 seconds cadence in relatively narrow (minimum) FoVs of 10 arcseconds wide. Inevitably, the polarimetric sensitivity needs to be reduced although the data can always be averaged to provide mean values with less temporal cadence.

[Goal 1.6] Flares and nano-flares energetics

Magnetic reconnection is a physical process where the involved magnetic fields can change their topology dramatically (fast reconnection) or in a more continuous way (slow reconnection). During the rearrangement, magnetic energy is mainly converted into kinetic (through acceleration of the particles or gas) and thermal (heating) energy. It is a fundamental physical process but its detailed characterization in nature has been elusive to researchers [Zweibel & Yamada 2009]. Reconnection events are hard to predict in the solar atmosphere and observations are very scarce. Several high spatial resolution observations (below 0.3") have shown clear evidences of reconnection events in high temperature plasmas, e.g., braiding structures [Cirtain et al. 2013]. But a detailed characterization of the involved energetics is still missing. Observations of the UV at a resolution of 0.3" and at temporal scales of 1 to 10 seconds can provide valuable information to understand the energy balance during small-scale reconnection events. High temporal and high sensitivity measurements will help detecting line asymmetries and high speed plasma flows as direct consequences of magnetic reconnection. Moreover, polarimetry can provide information about how the magnetic field lines reorganize after they reconnect what will bring unprecedented scientific progress to the understanding of reconnection processes in the solar chromosphere and TR. From active regions to small scale emergence events, the measurements shall be precise enough to allow the determination of flows, temperatures, densities and magnetic fields during and after reconnection events. Flows and heat resulting from reconnection events have not been quantitatively measured to date. The observations will help clarify fundamental open problems concerning magnetic reconnection.

4. Mission configuration

4.1. Mission profile

The preferred orbit is a low-Earth (LEO), Sun-synchronous orbit (SSO) such as in Hinode, IRIS or the PROBA missions at an altitude between 600 and 800 km. In an SSO orbit the spacecraft will point continuously to the Sun for about eight months without any eclipse periods. In this constant thermal environment the number of instrument calibrations can be reduced significantly. In this orbit and with a number of ground stations the data telemetry can be above 50 gigabits/day.

4.2. Payload

4.2.1. Baseline science instrument

While most of the scientific targets require high-spatial resolution for distinguishing elementary magnetic structures (~250 km or 0.3"), they also need information about the vector magnetic field which sets stringent conditions about the polarimetric sensitivity of the instrument and hence

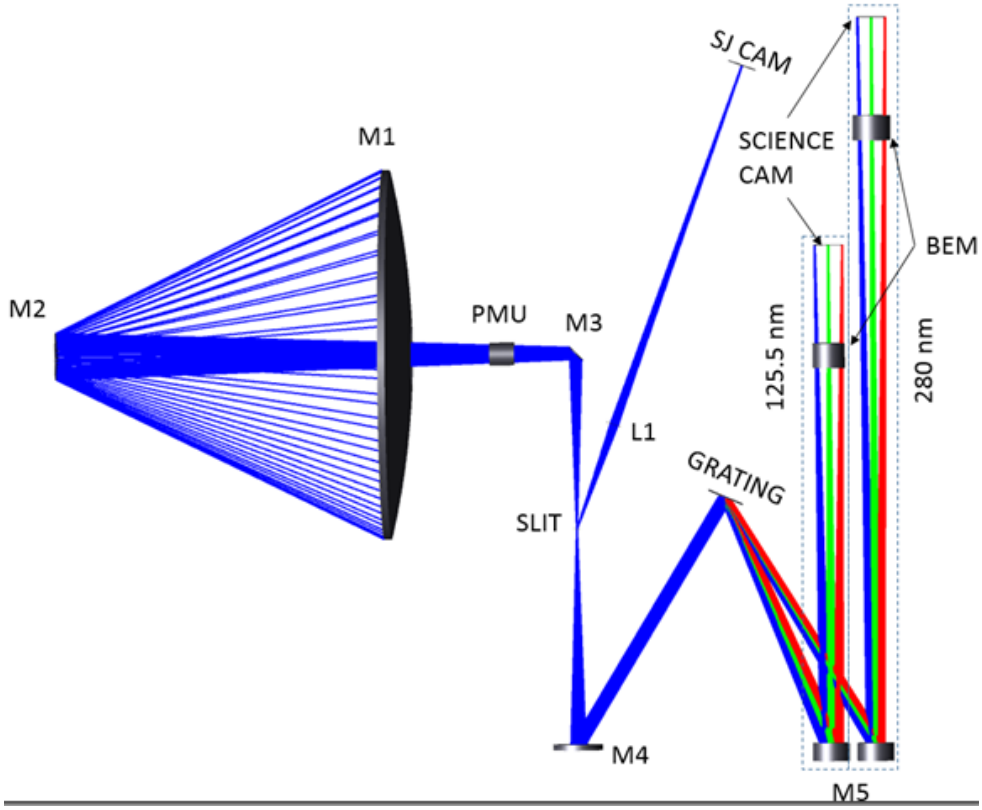

Figure 1: Instrumental layout of CASPER mission payload.

limits the spatial resolution. Since the discovery space is much larger for polarimetry, a limit resolution of about 0.4” in the Ly-alpha line at 121.567 nm and about 0.3” for the Mg II h&k seems to be a good compromise (Table 3)[3]. This sets the main telescope diameter and limits the number of intermediate optics to optimize the photon flux budget (see Section 4.2). The proposed CASPER mission instrument consists in an F/15 on-axis, axially symmetric, ∅30 cm primary mirror M1 Ritchey-Chrétien telescope, which feeds a conventional spectropolarimeter. The telescope forms an image of the Sun onto the entrance slit of the spectropolarimeter with a plate scale of 45"/mm and provides a diffraction[4] limited spatial resolution of about 0.10" at 121 nm and 0.23" at 280 nm. The instrument optical design is depicted in Figure 1. After M1, the beam reaches an active secondary, ∅4 cm mirror M2 with focus capabilities. The field stop is placed near M2 and limits the maximum FoV to 400”x400” in the slit-jaw channel and along the slit direction in the science focal planes. The beam hits later a flat mirror M3 which acts as the scan mirror mechanism for the spectrograph and as an active tip-tilt mirror for image stabilization [IS-SMM] (see Section 4.2). Then, the image is formed over the slit F1. The slit is integrated into an MS mirror that bounces back the light beam and form [after the L1 doublet and a narrow-band pass filter] an image of the scene around the slit into the slit-jaw camera system. In order to minimize the number of optical components and cameras, the slit-jaw camera is also part of the image stabilization system [ISS] (see Section 4.2).

The spectrograph is based in the common Czerny–Turner design, i.e., after the slit, the beam reaches a collimator mirror M4. The collimated light is diffracted by the grating onto the camera mirrors M5 that focus the two beams on two science focal planes, for both, the Mg II h&k and

[3] Achievable by pixel binning to reach the desired polarization sensitivity and by carefully selecting the spectrograph slit width, the grating groves and incident angles.

[4] Using the Rayleigh criterion.

the Ly-alpha lines at 280.270 nm and 121.567 nm. The spectrograph spectral bandwidth should be of, at least, 6 nm centered at the 121 nm and 280 nm reference wavelengths. The spatial sampling is limited to 0.22”/pixel at the 121 nm channel and to 0.15”/pixel at 280 nm to increase the throughput of the instrument and the slit FoV to about 400” and 450” for the two channels. The spectral sampling is 3.3 pm/px to deliver a final spectral resolution of around 10 pm in both channels with a grating of 2400 lines/mm working in order between 1 (Mg II h&k channel) and 2 (Ly-alpha channel). The spectrograph is outlined in Figure 1, where the main difference of the two channels is that each uses a dedicated camera mirror.

The two science detectors consist of a 2k x 2k thinned, back-illuminated sCMOS sensor with high quantum efficiency in the NUV and a pixel pitch of 11 micron which over-samples the spectral resolution by factor three. The camera frame rate should be, at least, 32 fps, for fulfilling the jitter and polarization sensitivity requirements. As an option, a third channel is devised, in this case, centered in the 390 nm spectral region. This channel would need just a third camera mirror and camera system plus the polarization analyzer.

Polarimetry will be done by placing a rotating wave-plate (polarization modulation unit; PMU) before the scan mirror mechanism in an F/15 beam which partly minimizes the angle deviations of the beam when going through the PMU. Two analyzer devices (e.g., a Wollaston) will be located in front of the two science detector and mounted in a mechanism to allow beam-exchange polarization (BEM), i.e., to alternatively measure the two orthogonal linear polarization components of the light beam in the same sensor area. Finally, the image stabilization system consists on a slit-jaw camera working as a *sensing* camera (i.e., to evaluate the jitter) and an active tip-tilt mirror using the spectrograph scan mirror mechanism [IS-SSM]. The ISS will be firmware based (see 4.3).

The system has a total of five moving parts, i.e., the M2 focus system, the PMU, the IS-SMM, and two BEMs, three cameras, seven reflective surfaces and two transmissive elements.

4.2.2. Instrument electronics

The mission electronics includes: a Data Processing Unit (DPU), an Analog, Motor and Heater Drivers board (AMHD), and a Power Converter Module (PCM). The DPU is the core of the instrument and has to be tailored such that it can perform data acquisition and accumulation, perform image stabilization tasks, image registering, demodulation and compression with a bitstream of around 2 GB/s, corresponding to the science detectors and the slit-jaw camera. The AMHD will be in charge of synchronizing the PMU and the BEM as well as taking care of the thermal stabilization of the more critical elements, among other analog tasks. The PCM is the direct interface to the platform and should hence fulfill the necessary requirements.

4.3. Mission viability

One, if not the most important, goal of the instrument is to reach a polarization sensitivity of the order of $3x10^{-4}$ in the UV. Classical polarimetric implementations suffer from systematic effects that limits the final polarimetric precision. Among them, the most important ones are: changes in the scenes during the **temporal modulation**, smearing due to “platform” **jitter**, the different **transmission** and optical **aberrations** of the two orthogonal polarizations (in the case of dual-beam) and finally, the **gain calibration** of the cameras which is often limited to 10^{-3}. Polarization cross-talk is likely to appear due to any of these systematic effects, spoiling the targeted polarization sensitivity of the instrument.

Table 2: Average transmission factors corresponding to main optical elements. 1) the slit-jaw camera includes a 1 nm transmission pass-band filter. 2) The transmission depends on the final crystal thickness.

	M1 ⌀30	M2 ⌀6	M3 [IS-SMM]	MS (flat)	L1 [SJS]1)	Grating +M4+M5	PMP2) and BEM2)	Total
Trans. [%]	~50 (120nm) >90 (290nm)	>75	>75	>75	~15 (120nm)	>75	~30 (120nm) ~ 90 (290nm)	**~1% (120nm)** **~6% (290nm)**
Coating	Cold mirror	Al + MgF_2	Al + MgF_2	Al + MgF_2	MgF_2	Al + MgF_2	MgF_2 / CaF_2	

Table 3: Estimated photon budget. Last two columns provide expected integration time needed for achieving two different polarization sensitivities for thee beam-exchange channels. The numbers can vary significantly depending on the final coatings, number of optical elements and polarization efficiency.

Photon Budget	Input Solar flux	At slit plane	At science plane	Spatial and spectral sampling	S/N single shot	Int. time for 10^{-3} polarimetric sensitivity	Int. time for $3x10^{-4}$ polarimetric sensitivity
	[ph/cm²/s/A/str]		[ph/s/"²]				
120 nm	7.3e15	2.0e15	4.1e3	0.44"/px 3 pm/px	30	**~45 sec**	**~9 min**
280 nm	1.7e16	8.5e15	2.4e4	0.3"/px 3 pm/px	140	**< 3 sec**	**~ 25 sec**

4.3.1. Dedicated jitter control

Image jitter during frame acquisition and polarization modulation can easily introduce polarization cross-talk signals in the demodulated data. In addition, any jitter also blurs the scene and decreases the amplitude of the polarization signals. The mission should carry dedicated instrumentation to mitigate the jitter effects. It should implement an attitude control system (ACS) to stabilize the image in the directions along the focal plane and in the angular direction. The ACS system will be used for pointing as well. The platform should also include star-trackers, solar limb sensors and a dedicated guiding telescope for proper position, attitude and maneuver determination.

The residual jitter will be corrected with an image stabilization system which uses the slit-jaw camera and the spectrograph scan mirror mechanism as the "sensing" and "corrector" devices. The image cross-correlation will be done in the system DPU. To reduce the jitter further, the science frames will be realigned before accumulation and before demodulation. This requires, among other things, to correct for dark current and flat-field on board, in order to properly shift the frames.

4.3.2. Polarization cross-talk control

The polarimetry is carried out using a rotating wave-plate and a polarizing beam-splitter that simultaneously sends two orthogonal polarization states (different linear combinations of the Stokes parameters) to the camera. This strategy, known as **dual-beam polarimetry**, is very efficient to remove the cross-talk signals generated by the temporal evolution of the scene and by the residual jitter. However, differential aberrations and transmission variations in the optics between

Table 4-5: Payload and mission phases for a total of 7,5 years of development plus mission exploitation

Payload phases

Phase	Dates (months)
Payload kick-off	T0 - 6
Phase 0 study	T0
Phase A/B	T0 + 24
Phase C (up to CDR)	T0 + 42
Phase D (up to delivery)	T0 + 72
Phase D+ (up to launch)	T0 + 90
Phase E (3 yr of nominal duration + 2 yr of mission extension)	T0 + 140

Mission phases

Phase	Dates (months)
Mission kick-off	T0
Phase 0 study	T0 + 6
Phase A/B industrial	T0 + 32
Phase C (up to CDR)	T0 + 51
Phase D (up to launch)	T0 + 90
Phase E (3 yr of nominal duration + 2 yr of mission extension)	T0 + 140

the two beams can introduce further spurious polarizations signals. Moreover, the camera gain strongly limits the achievable signal-to-noise ratio (S/N) in polarization. A powerful way to overcome such limitations consists in combining temporal and spatial polarization measurements, that is, the system sends first the two orthogonal polarization states to different areas of the detector and then "exchanges" the two beams and record them again. Of course, these operations should be synchronized with the modulator in order to have the same orientations of the retarder. This technique, known as "**beam-exchange**" polarimetry, is very powerful and provides enough information to reach, photon noise permitting, polarimetric sensitivities down to 10^{-5} [Elmore et al. 1992, Martinez Pillet et al. 1999; Collados 1999]. Finally, this technique allows to combine many exposures to increase the S/N further. The only limitation is that the frames need to be carefully aligned in order not to introduce additional spurious signals (see Section 4.2.1).

4.3.3. Dedicated flat-fielding strategy

Flat-field uncertainties (due to, e.g., camera gain) introduce spurious polarization signals, particularly in sCMOS detectors. To mitigate this problem we propose to calculate the flat-fields in two different ways: using the solar disk center and by averaging frames through the technique developed by Kuhn et al. (1991), i.e., moving the spectral images of the scientific cameras along the spatial direction (corresponding to the slit direction) using the scan-mirror mechanism and processing the data afterwards. This way, flat-fields can be taken at the same position of the observed solar scene what will minimize the impact of a different illumination into the science cameras in the data post-processing and in the polarization calibration.

4.3.4. Photon budget

All elements in the present design need to be made of special materials, for the case of transmissive optics, and coatings, for reflective surfaces, to ensure high throughput. There are not many coatings and transmission crystals with high throughput in the UV. Most of them are based on fluoride composites such as MgF_2 or CaF_2 birefringent materials. Table 2 summarizes the total transmission of the instrument with the respective baseline coatings or glass materials.

Table 6: Technology Readiness Level (TRL) of subsystems, heritage and leading country.

Instrument / key parts	Mission/instrument heritage	TRL now	Country of heritage
30 cm telescope	CLASP/Hinode/PHI/Sunrise	7	Germany/Spain/Japan
UV spectrograph	Sunrise-III/CLASP	7	Germany/Japan
E-Unit	Sunrise/PHI	9	Spain
Cameras	Sunrise-III	8	Spain
UV materials / coatings	Sunrise/CLASP/METIS	8	Spain/Japan/Italy
Mirrors	Sunrise	9	France
ISS firmware system	Lagrange	3	Spain
PMU	Sunrise/CLASP/Hinode	9	Japan
Scan mirror	Sunrise III	7	Japan
Thermal engineering and HW	Sunrise/PHI	9	Spain

Table 3 summarizes the photon budget calculation for the instrument and the achieved S/N ratios in polarization and the necessary effective integration times. The camera quantum efficiency (QE) varies very sharply in the UV. Current sCMOS sensors range from 30% QE in 120 nm to >45% in 290nm, depending on the coatings. With this configuration, the estimated integration time for achieving 10^{-3} and $3x10^{-4}$ polarization sensitivities goes from 45 second to 9 minutes, in the 120 nm range, to about 3 and 25 seconds at 290 nm. The expected integration times fulfill the main scientific requirements presented in Table 1.

5. Management structure

Payload and mission phases are identified in Tables 4 and 5. The timescale for total development is around 7.5 years from kick-off to launch plus a nominal mission duration of three years and two years of mission extension. The telescope and the instrument relay on existing technologies which have already flown in space of in rocket and balloon borne flights. Table 6 summarizes the Technology Readiness Level for mission key parts and main technology leading countries. Most technology have already been put in orbit (Hinode, PHI and METIS instruments onboard the Solar Orbiter mission and CLASP I and II experiments) or have flown (or plans to do so before 2022) in the Sunrise Ballon based observatory. The new ISS firmware based system that uses the slit-jaw camera as the “sensing” device and further realignment of images using the science camera is a proof-of-concept for the ESA Lagrange Missions Remote Sensing Instruments Phase A/B1 Study & Pre-developments. Verification of technologies for this mission can be done within 2-3 years.

5.1. Science operations

The mission includes the development of all on-ground data processing pipeline tools including data calibration and corrections as well as to yield Level 1 and Level 2 (“scientific” units”) data products to the scientific community. Obtaining level 2 data requires the interpretation of the

observed polarization signals with complex radiative transfer tools and the interpretation of atomic level polarization and the Zeeman and Hanle effects. The CLASP I and II rocket experiments have provided enough data to make these inference tools available to the solar community in due time.

5.2. Preliminary costs

A preliminary mission cost estimate has been evaluated using the heritage of previous missions such as Sunrise, PHI in Solar Orbiter and Lagrange. The costs can be found in Table 7, include the S/C development and the mission's nominal operations. The total cost is below the 150M€ envelop for small ESA missions. The cost excludes the member state contributions which will be responsible for the scientific payload and for the development of the data analysis tools necessary to yield level 2 data to the community.

Table 7: Preliminary costs

Concept	Cost (M€)
ESA project team	25
Industrial prime for platform	70
MOC & SOC	35
Margin (15 %)	19,5
Total	**149,5**

6. Bibliography

Alsina Ballester, Belluzi and Trujillo Bueno, 2016, ApJL, 831, 2

Alsina Ballester, Belluzi and Trujillo Bueno, 2017, ApJL, 836, 1

Alsina Ballester, Belluzi and Trujillo Bueno, 2018, ApJL, 854, 2

Alsina Ballester, Belluzi and Trujillo Bueno, 2019, ApJL, in press

Antolin et al., 2015, ApJ, 809, 1

Avrett et al. 2015, ApJ, 811, 2

Belluzzi and Trujillo Bueno, 2012, ApJL, 750, 1

Berger, Shine, Slater, et al. 2008, ApJL, 676, L89

Berger, Slater, Hurlburt, et al., 2010, ApJ, 716, 1288

Berger, Testa, Hillier, et al., 2011, Nature, 472, 197

Carlsson & Stein, 2002, ApJ, 572, 1

Centeno, Trujillo Bueno & Asensio Ramos, 2010, ApJ, 708, 1579

Chae, Ahn, Lim, Choe,& Sakurai, 2008, ApJL, 689, L73

Cirtain et al., 2013, Nature, 493, 7433

Collados, 1999, ASP Conf. Series, 184, 3-22. Eds. B. Schmieder, A. Hofmann, J. Staude

De Pontieu et al., 2004, Nature, 430, 6999

De Pontieu et al., 2007a, Science, 318, 5856

De Pontieu et al., 2007b, ApJ, 655, 1

De Pontieu et al. 2014, SoPh, 289, 7

Del Pino Alemán, Casini & Manso Sainz 2016, ApJ, 830, 24

Díaz Baso, Martínez González and Asensio Ramos, 2016, ApJ, 822, 50

Elmore et al., 1992, SPIE, A93-33401

Elmore et al., 2014, SPIE, 9147, 914707

Ermolli et al., 2013, ACP, 13, 8

Gòsic et al., 2016, ApJ, 820, 1

Gudiksen et al. 2011, A&A, 531, A154
Hillier, Berger, Isobe, & Shibata, 2012, ApJ, 746, 2
Kano et al., 2017, ApJL, 839, 1
Katsukawa et al., 2007, Science, 318, 5856
Khan et al., 2011, A&A, 529, 12
Kuhn, Lin, & Loranz, 1991, PASP, 103, 1097
Martínez Gonzalez & Bellot Rubio, 2009, ApJ, 700, 1391
Martínez Gonzalez et al., 2015, ApJ, 802, 3
Martínez Pillet et al., 1999, ASPC, 183, 264
Martínez-Sykora et al., 2017, Science, 356, 1269
Ni, Lukin, Murphy, & Lin, 2018, ApJ, 852, 95N
Okamoto et al., 2007, Science, 318,1577
Okamoto et al., 2015, ApJ, 809, 71O
Orozco Suárez, Asensio Ramos, & Trujillo Bueno, 2012, IAUS, 300, 112O
Orozco Suárez, Asensio Ramos, & Trujillo Bueno, 2015, ApJL, 803, L18
Ortiz et al., 2016, ApJ, 825, 93O
Pereira, De Pontieu, Carlsson, 2012, ApJ, 759, 18P
Pereira, Rouppe van der Voort, Carlsson, 2016, ApJ, 824, 65
Ryutova et al, 2010, SoPh, 267, 75R
Salz, Czesla, Schneider, Schmitt, 2016, A&A, 586, 75
Sekse, Rouppe van der Voort, De Pontieu, 2012, ApJ, 752, 108
Sekse, Rouppe van der Voort, De Pontieu, 2013, ApJ, 764, 164
Štěpán, Trujillo Bueno, Leenaarts, & Carlsson, 2015, ApJ, 803, 65
Tavabi, Koutchmy, Ajabshirizadeh, 2011, NewA, 16, 296
Trujillo Bueno, et al., 2018, ApJ, 866, 15
Trujillo Bueno, Landi Degl'Innocenti & Belluzzi, 2017, SSRv, 210, 183
Trujillo Bueno, Štěpán, & Casini, 2011, ApJL, 738, 1
Trujillo Bueno 2011, ASPC, 437 83
Zweibel & Yamada, ARA&A, 47, 291